GEOLOGY | THE GEOLOGICAL SOCIETY OF AMERICA®

https://doi.org/10.1130/G47172.1

Manuscript received 5 November 2019
Revised manuscript received 28 February 2020
Manuscript accepted 8 March 2020

Radioisotopic and biostratigraphic constraints on the classical Middle–Upper Permian succession and tetrapod fauna of the Moscow syneclise, Russia

V.I. Davydov[1,2], M.P. Arefiev[2,3], V.K. Golubev[2,4], E.V. Karasev[2,4], M.A. Naumcheva[4], M.D. Schmitz[1], V.V. Silantiev[2] and V.V. Zharinova[2]

[1]Department of Geosciences, Boise State University, Boise, Idaho 83725, USA
[2]Institute of Geology and Petroleum Technology, Kazan Federal University, 18 Kremlyovskaya Street, Kazan, Republic of Tatarstan 420008, Russia
[3]Geological Institute of Russian Academy of Sciences, Pyzhevsky lane 7, Moscow 119017, Russia
[4]Borissiak Paleontological Institute of the Russian Academy of Sciences, Profsoyuznaya 123, Moscow 117647, Russia

ABSTRACT

The East European Platform and the PreUrals are the regions where the Permian System was first established, but the provincialism of fossils and lack of radioisotopic age control have prevented the use there of the regional Permian subdivisions used outside of the region. We report the first U-Pb zircon chemical abrasion–isotope dilution–thermal ionization mass spectrometry (CA-ID-TIMS) age of 253.95 ± 0.06 Ma for a volcanic tuff from the terrestrial upper part of the lower Vyatkian Regional Stage in the Moscow syneclise (Russia). This age greatly improves the correlation of the East European Platform and the PreUrals with the international geologic time scale, and contributes to our understanding of sedimentation within the Permian-Triassic transition in the studied region. The new radioisotopic age integrated within the regional chronostratigraphic framework reveals the synchrony in extinction of faunas of the Dinocephalian superassemblage in the studied region with that in South Africa.

INTRODUCTION

The East European Platform and PreUrals (western flanks of the Ural Mountains) (EEPP) is the type region of the Permian System (Murchison et al., 1845). In addition to the historical priority, the successions are famously rich in faunas of tetrapods (Amalitzky, 1922; Efremov and V'yushkov, 1955; Golubev, 2000; Tverdokhlebov et al., 2005). Excellent preservation, substantial diversity, and excellent stratigraphic constraints on the tetrapods within a regional chronostratigraphic framework (Arefiev et al., 2015) denote a key role for this fauna in our understanding of the evolution of tetrapods (Benton, 2015; Lucas, 2017). At the same time, the provincial temperate faunas in the EEPP section are of limited global chronostratigraphic value, and thus the temporal correlation of the tetrapod communities of the EEPP within the global context is still controversial.

A significant hiatus in sedimentation (6–9 m.y.) across the Permian-Triassic transition of the EEPP was proposed in the 2012 Geologic Time Scale (GTS; Gradstein et al., 2012), with all or most of the Lopingian Series missing (Henderson et al., 2012). This gap was an assumption from earlier and recent studies (Lozovskiy and Esaulova, 1998; Tverdokhlebov et al., 2005). Today, many geologists consider the Permian–Triassic continental succession in the EEPP as more complete (Arefiev et al., 2015; Sennikov and Golubev, 2017; Scholze et al., 2019). The regional biostratigraphy, including data on nonmarine ostracods and bivalves, tetrapods, conchostracans (clam shrimp), fish remains, and plants, along with magnetostratigraphy and chemostratigraphy, provide a reliable regional chronostratigraphic framework (Taylor et al., 2009; Newell et al., 2010; Golubev, 2015; Scholze et al., 2019; Naumcheva and Golubev, 2020). We have discovered a volcanic ash bed and obtained the first ever high-precision chemical abrasion–isotope dilution–thermal ionization mass spectrometry (CA-ID-TIMS) age in the entire Middle-Upper Permian of the EEPP from the upper part of the lower Vyatkian Regional Stage in the Sukhoborka locality at Vetluga River, Nizhny-Novgorod region, Russia (Fig. 1). We integrated this volcanic ash within the regional chronostratigraphic framework and made several observations regarding completeness of the studied sedimentary succession, correlation with the 2012 GTS, the evolution of tetrapods, and climate.

GEOLOGICAL SETTING

The continental Permian–Triassic sequences in the Moscow syneclise are best exposed along the Sukhona and Malaya Severnaya Dvina Rivers of the Vologda region, and along the Vetluga River in the Nizhny-Novgorod region (Fig. 1; Arefiev et al., 2015). The Upper Permian–Lower Triassic is divided into series of formations that are successively exposed along the rivers (Fig. 1). The lithostratigraphy and biostratigraphy of the succession in the region are well established (Arefiev et al., 2015) and provide a precise correlation with other sections within the Moscow syneclise. The Vyatka Formation in the region is divided (upward) into the Zamoshnikovo, Luptug, and Moloma Members (Fig. 1; see Fig. S3 in the Supplemental Material[1]). The formation overlies the silty limestone of the

[1]Supplemental Material. Figures S1–S4 (photos, stratigraphic logs, stratigraphy, and results of single grain chemical abrasion ID-TIMS analysis) and Tables S1 and S2 (fossils, and U-Pb isotopic data). Please visit https://doi.org/10.1130/GEOL.26213S.12132822 to access the supplemental material, and contact editing@geosociety.org with any questions.

CITATION: Davydov, V.I., et al., 2020, Radioisotopic and biostratigraphic constraints on the classical Middle–Upper Permian succession and tetrapod fauna of the Moscow syneclise, Russia: Geology, v. 48, p. , https://doi.org/10.1130/G47172.1

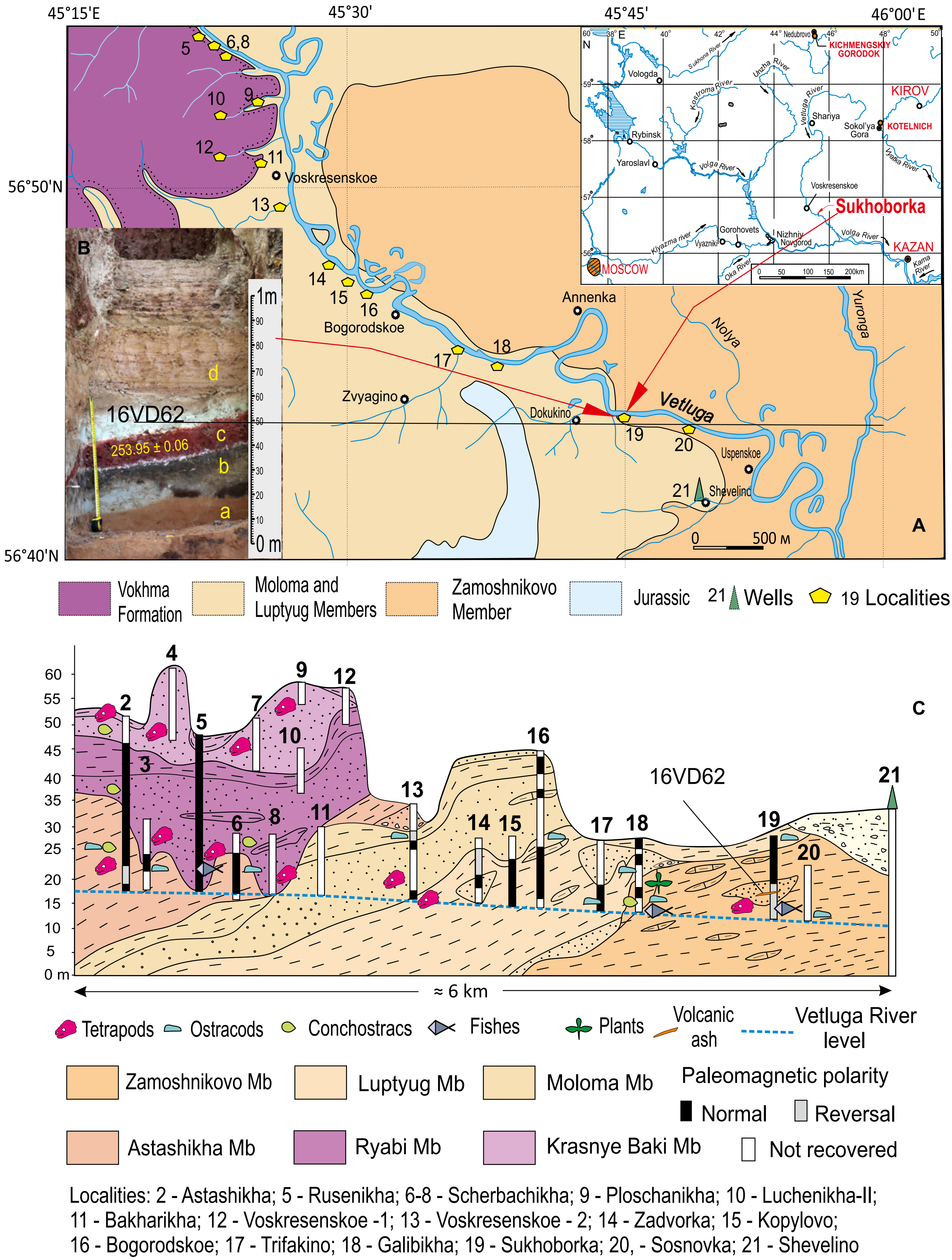
45°15'E
45°30'
45°45'
46°00'E
56°50'N
56°40'N
A
B
C
Voskresenskoe
Bogorodskoe
Annenka
Zvyagino
Dokukino
Uspenskoe
Shevelino
Vetluga
Nolya
Yuronga
500 м
Sukhoborka
MOSCOW
KAZAN
KIROV
KOTELNICH
KICHMENGSKIY GORODOK
16VD62
253.95 ± 0.06
1m
0 m
Vokhma Formation
Moloma and Luptyug Members
Zamoshnikovo Member
Jurassic
21 Wells
19 Localities
≈ 6 km
Tetrapods
Ostracods
Conchostracs
Fishes
Plants
Volcanic ash
Vetluga River level
Zamoshnikovo Mb
Luptyug Mb
Moloma Mb
Astashikha Mb
Ryabi Mb
Krasnye Baki Mb
Paleomagnetic polarity
Normal
Reversal
Not recovered
Localities: 2 - Astashikha; 5 - Rusenikha; 6-8 - Scherbachikha; 9 - Ploschanikha; 10 - Luchenikha-II;
11 - Bakharikha; 12 - Voskresenskoe -1; 13 - Voskresenskoe - 2; 14 - Zadvorka; 15 - Kopylovo;
16 - Bogorodskoe; 17 - Trifakino; 18 - Galibikha; 19 - Sukhoborka; 20, - Sosnovka; 21 - Shevelino

Figure 1. Geologic map and cross section of the Sukhoborka study area, Vetluga River, Nizhny-Novgorod region, Russia. (A) Geologic map (sheet O38-XXVIII by G.I. Blom, unpublished, 1964) with main localities mentioned in the text. (B) Close-up of discovered volcanic ash bed at Sukhoborka; *a*—brownish-light slightly reddish, poorly laminated fine sandstone; *b*—greenish-gray to bluish, poorly laminated fine sandstone with black lenses enriched in organic matter; *c*—strongly crimson volcanic ash bed with sharp lower and upper contacts; *d*—fine sandstone similar to *a*. (C) Cross section with general logs and paleomagnetic data of main localities mentioned in text (modified from Lozovskiy and Esaulova, 1998). Paleomagnetic data are from Balabanov and Muraviev (2010) and Lozovskiy et al. (2015). Biostratigraphy for each locality is provided in the Supplemental Material (see footnote 1).

Wuchiapingian Putyatinian Formation and is overlapped by the Triassic Vokhma Formation. The Sukhoborka location occurs in the lower course of the Vetluga River (Fig. 1).

MATERIAL, METHODS, AND RESULTS

An altered volcanic ash bed (bentonite) was found at the Sukhoborka section (56.73094°N, 45.74826°E), in the middle part of the Zamoshnikovo Member, which is composed of floodplain to lacustrine, sandy to silty, sediments, often with paleosol horizons (Lozovskiy and Esaulova, 1998). The bentonite is located within sandstone of the Zamoshnikovo Member, 6 m above the Vetluga River bottom at Sukhoborka, and ~15 m above the regional base of the member (Fig. 1). The bentonite is 7–13 cm thick (bed C in Fig. 1) and occurs immediately above a greenish-gray fine sandstone with black lenses enriched in organic matter (beds A–B in Fig. 1). The appearance of the latter suggests a low-energy, and possibly local stagnant, slackwater environment, where the volcanic material at this locality was preserved. The Sukhoborka ash bed, according to faunal data from strata below and above these beds (Fig. 1; Figs. S2 and S3, Table S1, and supplemental text), correlates with the upper Bykovian Regional Substage (RS) of the lower Vyatkian Regional Stage (Figs. 1 and 2; Arefiev et al., 2015).

Sample 16VD62 from bed C at the Sukhoborka locality yielded hundreds of sharply facetted, elongate, prismatic zircon crystals (Fig. S1), from which we selected eight single zircon grains for dating. All analyses yielded concordant and equivalent isotope ratios, and these were combined to yield a weighted mean $^{206}Pb/^{238}U$ date of 253.95 ± 0.06(0.14) [0.30]

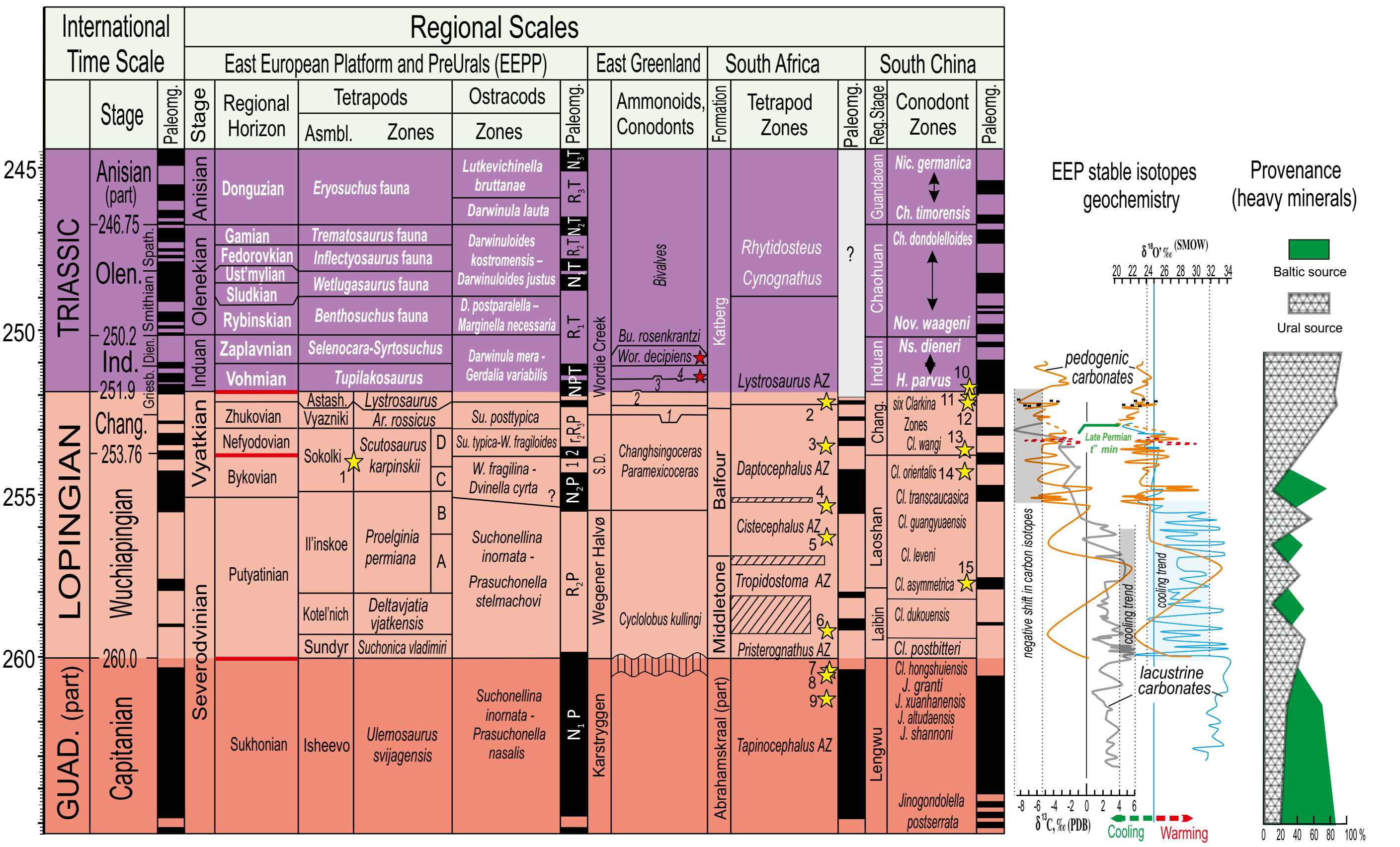

★ **Dated volcanic ashes: 1**, 253.95; **2**, 252.24; **3**, 253.48; **4**, 255.2; **5**, 256.25; **6**, 259.26; **7**, 260.26; **8**, 260.41; **9**, 261.24; **10**, 251.88; **11**, 251.94;**12**, 252.36; **13**, 253.60; **14**, 254.31; **15**, 257.79

Faunistic abbreviations: Ar. – *Archosaurus*. Ostracods: *D. - Darwinula*; *G. – Gerdalia*, *Su. – Suchonella*, *W. - Wjatkellina*. Conodonts: *Cl. – Clarkina*; *H. – Hindeodus*; *J. – Jinogondolella*; *Ns. – Neospathodus*; *Nov. – Novispathodus*; *Ch. – Chiosella*; *Nic. – Nicoraella*. **Biozones in Greenland**: 1, *Otoceras concavum - Hypophiceras triviale*; 2, *Otoceras boreale - Metophiceras subdemissum*; 3, *Tompophiceas pascoei - Hindeodus parvus*; 4, *Ophiceras commune* (Kozur, 1998; Bjerager et al., 2006). *Wor. - Wordieoceras*; *Bu. - Bukkenites.* ★ *Tupilakosaurus* fauna in Greenland. P/m chrons in EEPP: 1 - r_1R_3P; 2 - n_1R_3P.

Figure 2. Correlation of the Permian-Triassic transition of the East European Platform and PreUrals (EEPP), East Greenland, South Africa, and south China. Three thick red lines within the EEPP succession are the level of the most reliable correlation with the 2012 Geologic Time Scale (Gradstein et al., 2012; Henderson et al., 2012). Paleomagnetic scale is from Hounslow and Balabanov (2018). EEPP tetrapod zones are from Sennikov and Golubev (2017); ostracod zonation and stable isotopic data and interpretations are from Arefiev et al. (2015). Regional chronostratigraphy, radioisotopic ages, and tetrapod zonation in South Africa are from Day et al. (2015); paleomagnetic data are from Tohver (2015), Lanci (2015), and Gastaldo (2018). Regional chronostratigraphy, zonation, and radioisotopic ages in south China are from Yuan et al. (2019). Astash.—Astashikha; GUAD.—Guadalupian; Chang.—Changhsingian; Ind.—Induan; Olen.—Olenekian; Griesb.—Griesbachian; Dien.—Dienerian; Spath.—Spathian. Tetrapod zones: A—*Chroniosaurus dongusensis*; B—*Chroniosaurus levis*; C—*Jarilinus mirabilis*; D—*Chroniosuchus paradoxus*. Provenance data are from Arefiev et al. (2011). PDB—Peedee belemnite; SMOW—standard mean ocean water.

Ma (2σ; mean square of weighted deviates [MSWD] = 1.44; $n = 8$), where the quoted errors indicate the following analytical uncertainties: (analytical + tracer), [analytical + tracer + decay constant]. This date is interpreted as estimating the volcanic eruption and depositional age. The narrow range in Th/U in the analyzed zircon crystals lends credibility to the interpretation that they are from a single source (Table S2; Fig. S4).

DISCUSSION

The new U-Pb zircon CA-ID-TIMS radioisotopic age from the upper Bykovian RS provides direct and precise correlation of the Lopingian rocks of the Moscow syneclise with the GTS (Fig. 2; Davydov et al., 2018; Yuan et al., 2019). Three chronostratigraphic levels constrain the Upper Permian–Lower Triassic successions in the EEPP (thick red lines on Fig. 2). The first level, the local Sukhonian-Putyatinian boundary, is associated with the main biotic and climate perturbation within the Middle Permian–Early Triassic in the region, as recorded in the evolution of tetrapods (Golubev, 2015), ostracods (Molostovskaya et al., 2018), fishes (*Platysomus-Toyemia* superassemblage boundary; Arefiev et al., 2015), and stable isotopes (δ^{13}C and δ^{18}O) of lacustrine carbonates (Fig. 2).

The carbon stable isotopes in lacustrine carbonates at the Capitanian-Wuchiapingian boundary demonstrate a significant shift toward heavier values, from 3‰ to 6‰, indicating a climatic cooling trend (Fig. 2). The oxygen isotopic composition of lacustrine carbonates in the Sukhonian RS possess relatively stable values, varying around 32‰–34‰, whereas starting from the Putyatinian RS, the oxygen isotopic compositions strongly oscillate between 22‰ and 32‰, also indicating a cooling trend (Fig. 2). The switch in mode is interpreted here as related to a prominent cooling and perturbation of the climate in the region (Leng and Marshall, 2004) during the late Capitanian–Wuchiapingian (Arefiev et al., 2015), and correlated to the global latest Capitanian–Wuchiapingian climatic perturbation established in Australia and elsewhere (Wignall et al., 2009; Metcalfe et al., 2015; Davydov et al., 2018). The switch in the stable isotopic data in the Moscow Basin was likely not caused by a change in provenance, as the input from the source in the Urals appears much earlier than the Capitanian-Wuchiapingian boundary proposed here (Arefiev et al., 2011). This input smoothly increased through the boundary and became dominant in post-Wuchiapingian time (Fig. 2).

Also near this chronostratigraphic level, the Capitanian paleomagnetic N_1P zone of the EEPP (Fig. 2) is interpreted to correlate with the upper Capitanian paleomagnetic records of west Texas (USA) and the uppermost Abrahamskraal Formation in South Africa (Hounslow and Balabanov, 2018). The numerical age of the latter is constrained by U-Pb zircon geochronology in west Texas (Ramezani and Bowring, 2018) and in the Abrahamskraal Formation (Day et al., 2015). Consequently, the paleomagnetic R_2P zone of EEPP correlates with the Wuchiapingian of the 2012 GTS (Fig. 2).

Drastic changes in tetrapod faunas occurred as a multistadial process of dinocephalian extinction around the mid-Severodvinian in the EEPP (late Sukhonian through early Putyatinian). The dinocephalian-dominated fauna of the *Ulemosaurus svijagensis* assemblage zone (AZ) was replaced by a pareiasaur, dicynodont, and theriodont–dominated fauna (*Suchonica vladimiri* AZ [transitional] and *Deltavjatia vjatkensis* AZ). The last single taxon of dinocephalian Ulemosauridae gen. indet. is found in the *Suchonica vladimiri* AZ (Golubev, 2015; Golubev and Bulanov, 2018). Similarly, in South Africa, the last dinocephalian *Criocephalosaurus* is found in the transition between the mass extinction of dinocephalians and immediately below the *Pristerognathus* AZ (Day et al., 2015). Apparently, the *Suchonica vladimiri* AZ has the same stratigraphic position as the uppermost *Tapinocephalus* AZ and *Pristerognathus* AZ in South Africa. The latter AZ is designated there as an "interval zone" between the last appearance of dinocephalians and the first appearance of the dicynodont *Tropidostoma* (Day et al., 2015). The *Pristerognathus* AZ, according the new radioisotopic ages in South Africa, correlates with the Wuchiapingian Stage of the 2012 GTS (Day et al., 2015), and thus the *Suchonica vladimiri* AZ in the EEPP also corresponds to the Wuchiapingian Stage (Fig. 2), although the uppermost Capitanian age of the lower *Suchonica vladimiri* AZ cannot be excluded.

The second constrained chronostratigraphic level within the Lopingian in the EEPP is the new CA-ID-TIMS age that we obtained from the Sukhoborka locality. It is ~200 k.y. older than the estimated radioisotopic age of the base of the Changhsingian in south China (Yuan et al., 2019). This suggests the correlation of the base of the Nefyodovian RS of the EEPP with the Wuchiapingian-Changhsingian boundary of the 2012 GTS (Fig. 2).

The third chronostratigraphic level of global utility, at the base of the Ryabi member of the Vokhmian RS (*Tupilakosaurus* AZ), possesses a direct biostratigraphic correlation with the Greenland *Tupilakosaurus* AZ (Fig. 2; Lozovskiy, 1967; Lucas, 2017; Novikov, 2018). This tetrapod fauna in Greenland first occurs in the lower *Ophiceras commune* ammonoid zone (Nielsen, 1954; Bjerager et al., 2006). The index species of the base of the global Triassic *Hindeodus parvus* in the region has been found with ammonoids *Hypophiceras*, *Tompophiceras gracile* (Spath), and *T. pascoei* (Spath) (Kozur, 1998) and slightly below *Tupilakosaurus*. According to the recent high-resolution $\delta^{13}C_{org}$ isotopic data, the first negative spike that is associated with the Permian-Triassic boundary (PTB) in south China occurs immediately below *Ophiceras commune* (Sanson-Barrera et al., 2015), which is consistent with the conodont and other ammonoid data (Fig. 2). The ammonoids, conodonts, and $\delta^{13}C_{org}$ isotopes in Siberia and Canada also suggested an Early Triassic age for the *Ophiceras commune* ammonoid zone of Greenland (Kozur, 1998; Algeo et al., 2012; Zakharov et al., 2015).

In the uppermost Permian, the first local occurrence datum of *Lystrosaurus blomi* from Vetluga (Blom, 1968) is in the lower Astashikha member of the lower Vokhmian RS of the EEPP. Originally, the Astashikha beds were included in the Permian (Blom, 1968). The discovery of *Lystrosaurus* in this unit, and common acceptance of the PTB in continental sequences at the first appearance datum (FAD) of the genus in South Africa, subsequently led some workers to equate the PTB in the EEPP to the base of Astashikha member (Lozovskiy and Esaulova, 1998). However, the occurrence of the reverse polarity chron within the lower Astashikha member (Fig. 2) as well as relatively low values of magnetic susceptibility and natural remanent magnetization (Lozovskiy et al., 2015) suggest a latest Permian age for the member. This interpretation is also supported by the negative shift in the carbon stable isotope record (Fig. 2; Arefiev et al., 2015), which correlates with a similar shift in the latest Permian in south China (Yuan et al., 2019). The ostracods from the Astashikha member belong to the *Darwinula mera–Gerdalia variabilis* ostracod AZ, which that correlates with the uppermost Permian–lowermost Triassic of the 2012 GTS (Naumcheva and Golubev, 2020). Finally, our new bentonite age in the analogues of the *Scutosaurus karpinskii* zone of the EEPP is consistent in biostratigraphic position and numerical age with a volcanic ash bed date in the *Dicynodon* Zone and near the base of the *Lystrosaurus* Assemblage Zone in South Africa reported by Gastaldo et al. (2015, 2020).

The integrated biostratigraphic, geochronologic, and paleomagnetic data in the Moscow syneclise presented here suggest the lack of a meaningful temporal gap in sedimentation across the Late Permian and into the P-T transition in the EEPP. The stratigraphic correlations proposed here greatly improve the reliability of regional to global correlation and expand our knowledge on paleoclimate change and tetrapod evolutionary processes within the Lopingian-Triassic transition in the region. Specifically, the base of the Putyatinian RS coincides with the extinction of the Dinocephalian tetrapod fauna in the EEPP (Golubev, 2015). A similar event, i.e., 74%–80% loss of tetrapod generic richness, mostly due to the extinction of all dinocephalian therapsids at the Capitanian-Wuchiapingian transition, is also observed in South Africa (Fig. 2; Day et al., 2015). The correlation proposed here finally resolves the problem of asynchrony between Permian tetrapod fauna extinction in Gondwana (South Africa and surrounding regions) and in Eurasian continents (EEPP and China) (Benton, 2012; Day et al., 2015; Lucas, 2017). We proposed that the extinction was associated with the P4 glaciation in eastern Gondwana (Metcalfe et al., 2015; Davydov et al., 2018) and potentially could have been caused by this climatic deterioration in temperate latitudes.

We suggest that the link between Emeishan basalt volcanism and the late Capitanian–Wuchiapingian extinction is precarious because this volcanism was generally post-Capitanian in age (ca. 260 Ma; Huang et al., 2016; Bagherpour et al., 2018; Li et al., 2018; Yang et al., 2018). The Capitanian-Wuchiapingian boundary is established at the base of bed 6k in the Penglaitan section in south China (Jin et al., 2006), and not at the beginning of Emeishan volcanism, as considered in some studies (Zhong et al., 2014; Day et al., 2015; Yang et al., 2018). Quantitative biostratigraphic constraints suggest a 260 Ma age for the boundary (Henderson et al., 2012). Nevertheless, the radioisotopic calibration of the Capitanian-Wuchiapingian boundary in the 2012 GTS still requires improvement.

ACKNOWLEDGMENTS

This work was supported by the Russian Scientific Foundation, project no. 19–17–00178 by the Ministry of Science and High Education of the Russian Federation contract No. 14.Y26.31.0029 in the framework of the Resolution No.220 of the Government of the Russian Federation (to Davydov, Karasev, and Silantiev); by the Russian Foundation for Basic Research, projects 17–04–00410, 17–54–10013, and 18–05–00593 (to Golubev) and 18–34–00721 (to Naumcheva); and by the subsidy of the Russian government to support the Program of Competitive Growth of Kazan Federal University (to all, except Schmitz). The study was carried out following the plans of the scientific research of the Geological Institute (Moscow) of Russian Academy of Sciences (No. 0135-2019-0073, Arefiev). We greatly appreciate the help of A. Bakaev, Ph.D. student of the Paleontological Institute, Moscow, for fossil fish identification; A. Ul'yakhin, Ph.D. student of Lomonosov Moscow State University, Moscow, for geological exploration of the Sukhoborka area; and W.S. Snyder, Boise State University (Idaho, USA), for critical comments on the manuscript. The comments and remarks of three anonymous reviewers helped to improve the manuscript.

REFERENCES CITED

Algeo, T., et al., 2012, Evidence for a diachronous Late Permian marine crisis from the Canadian Arctic region: Geological Society of America Bulletin, v. 124, p. 1424–1448, https://10.1130/B30505.1.

Amalitzky, V.P., 1922, Diagnoses of the new forms of vertebrates and plants from the Upper Permian of North Dvina: Bulletin de l'Académie des Sciences de Russie, v. 22, p. 329–340.

Arefiev, M.P., Shkurskii, B.B., and Grigorieva, A.V., 2011, The influence of Baltic and Ural provincial sources on the sedimentation around Permian-Triassic transition in the north-east part of the Moscow syneclise, *in* Yapaskurt, O.V., et al., eds., The Conceptual Problems of Lithological Investigations in Russia: Kazan, Kazan Federal University, p. 63–67 [in Russian].

Arefiev, M.P., Golubev, V.K., Balabanov, Y.P., Karasev, E.V., Minikh, A.V., Minikh, M.G., Molostovskaya, I.I., Yaroshenko, O.P., and Naumcheva, M.A., 2015, Type and Reference Sections of the Permian–Triassic Continental Sequences of the East European Platform: Stable Isotopes, Paleomagnetic, and Biotic Events: Moscow, Paleontological Institute of the Russian Academy of Sciences, 99 p.

Bagherpour, B., Bucher, H., Yuan, D.-X., Leu, M., Zhang, C., and Shen, S.-z., 2018, Early Wuchiapingian (Lopingian, Late Permian) drowning event in the South China block suggests a late eruptive phase of Emeishan large igneous province: Global and Planetary Change, v. 169, p. 119–132, https://doi.org/10.1016/j.gloplacha.2018.07.013.

Balabanov, Y.P., and Muraviev, F.A., 2010, Results of paleomagnetic studies of the Permian and Triassic transition in Vetluga and Kichmenga Rivers, *in* Golubev, V.K., and Sennikov, A.G., eds., Permian and Triassic Paleontology and Stratigraphy of North Eurasia: Materials of the 5th International Conference devoted to the 150th Anniversary of Vladimir Prokhorovich Amalitzky (1860–1917): Moscow, Paleontological Institute of the Russian Academy of Sciences, p. 45–48 [in Russian].

Benton, M.J., 2012, No gap in the Middle Permian record of terrestrial vertebrates: Earth-Science Reviews, v. 40, p. 339–342, https://doi.org/10.1130/G32669.1.

Benton, M.J., 2015, Vertebrate Palaeontology (4th ed.): Chichester, UK, Wiley-Blackwell, 486 p.

Bjerager, M., Seidler, L., Stemmerik, L., and Surlyk, F., 2006, Ammonoid stratigraphy and sedimentary evolution across the Permian-Triassic boundary in East Greenland: Geological Magazine, v. 143, p. 635–656, https://doi.org/10.1017/S0016756806002020.

Blom, G.I., 1968, Catalog of Fossil Localities in the Lower Triassic of Middle Povolzhie and Prikamie: Kazan, Russia, Kazan State University, 386 p. [in Russian].

Davydov, V.I., Biakov, A.S., Schmitz, M.D., and Silantiev, V.V., 2018, Radioisotopic calibration of the Guadalupian (middle Permian) series: Review and updates: Earth-Science Reviews, v. 176, p. 222–240, https://doi.org/10.1016/j.earscirev.2017.10.011.

Day, M.O., Ramezani, J., Bowring, S.A., Sadler, P.M., Erwin, D.H., Abdala, F., and Rubidge, B.S., 2015, When and how did the terrestrial mid-Permian mass extinction occur? Evidence from the tetrapod record of the Karoo Basin, South Africa: The Royal Society Proceedings: ser. B, Biological Sciences, v. 282, 20150834 , https://doi.org/10.1098/rspb.2015.0834.

Efremov, I.A., and V'yushkov, B.P., 1955, Catalogue of Localities of Permian and Triassic Terrestrial Vertebrates in the Territories of the U.S.S.R.: Moscow, Academy of Sciences of USSR Publishing House, 185 p. [in Russian].

Gastaldo, R.A., Kamo, S.L., Neveling, J., Geissman, J.W., Bamford, M., and Looy, C.V., 2015, Is the vertebrate-defined Permian-Triassic boundary in the Karoo Basin, South Africa, the terrestrial expression of the end-Permian marine event?: Geology, v. 43, p. 939–942, https://doi.org/10.1130/G37040.1.

Gastaldo, R.A., Neveling, J., Geissman, J.W., and Kamo, S.L., 2018, A lithostratigraphic and magnetostratigraphic framework in a geochronologic context for a purported Permian-Triassic boundary section at Old (West) Lootsberg Pass, Karoo Basin, South Africa: Geological Society of America Bulletin, v. 130, p. 1411–1438, https://doi.org/10.1130/B31881.1.

Gastaldo, R.A., Kamo, S.L., Neveling, J., Geissman, J.W., Looy, C.V., and Martini, A.M., 2020, The base of the *Lystrosaurus* Assemblage Zone, Karoo Basin, predates the end-Permian marine extinction: Nature Communications, v. 11, p. 1428, https://doi.org/10.1038/s41467-020-15243-7.

Golubev, V.K., 2015, Dinocephalian stage in the history of the Permian tetrapod fauna of Eastern Europe: Paleontological Journal, v. 49, p. 1346–1352, https://doi.org/10.1134/S0031030115120059.

Golubev, V.K., and Bulanov, V.V., 2018, Amphibians of the Permian Sundyr Tetrapod Assemblage of Eastern Europe: Paleontological Journal, v. 52, p. 639–652, https://doi.org/10.1134/S0031030118060059.

Golubev, V.K., 2000, Permian and Triassic Chroniosuchians and tetrapod biostratigraphy of the upper Tatarian deposits of Eastern Europe: Transactions of Paleontological Institute of the Russian Academy of Sciences, v. 276, p. 1–174 [in Russian].

Gradstein, F., Ogg, J.G., Schmitz, M., and Ogg, G., 2012, The Geologic Time Scale 2012: Amsterdam, Elsevier, 1176 p., https://doi.org/10.1016/C2011-1-08249-8.

Henderson, C., Davydov, V.I., and Wardlaw, B.R., 2012, The Permian Period, *in* Gradstein, F.M., et al., eds., The Geologic Time Scale 2012: Amsterdam, Elsevier, p. 653–679, https://doi.org/10.1016/B978-0-444-59425-9.00024-X.

Hounslow, M.W., and Balabanov, Y.P., 2018, A geomagnetic polarity timescale for the Permian, calibrated to stage boundaries, *in* Lucas, S.G., and Shen, S., eds., The Permian Timescale: Geological Society [London] Special Publication 450, p. 61–103, https://doi.org/10.1144/SP450.8.

Huang, H., Cawood, P.A., Hou, M.-C., Yang, J.-H., Ni, S.-J., Du, Y.-S., Yan, Z.-K., and Wang, J., 2016, Silicic ash beds bracket Emeishan large igneous province to <1 m.y. at ~260 Ma: Lithos, v. 264, p. 17–27, https://doi.org/10.1016/j.lithos.2016.08.013.

Jin, Y.G., Shen, S.Z., Henderson, C.M., Wang, X.-D., Wang, W., Wang, Y., Cao, C., and Shang, Q., 2006, The global stratotype section and point (GSSP) for the boundary between the Capitanian and Wuchiapingian Stage (Permian): Episodes, v. 29, p. 253–262, https://doi.org/10.18814/epiiugs/2006/v29i4/003.

Kozur, H.W., 1998, Problems for evaluation of the scenario of the Permian -Triassic boundary biotic crisis and of its causes: Geologia Croatica, v. 51, no. 2, p. 135–162.

Lanci, L., Tohver, E., Wilson, A., and Flint, S., 2013, Upper Permian magnetic stratigraphy of the lower Beaufort Group, Karoo Basin: Earth and Planetary Science Letters, v. 375, p. 123–134, https://doi.org/10.1016/j.epsl.2013.05.017.

Leng, M.J., and Marshall, J.D., 2004, Palaeoclimate interpretation of stable isotope data from lake sediment archives: Quaternary Science Reviews, v. 23, p. 811–831, https://doi.org/10.1016/j.quascirev.2003.06.012.

Li, Y., He, H., Ivanov, A.V., Demonterova, E.I., Pan, Y., Deng, C., Zheng, D., and Zhu, R., 2018, $^{40}Ar/^{39}Ar$ age of the onset of high-Ti phase of the Emeishan volcanism strengthens the link with the end-Guadalupian mass extinction: International Geology Review, v. 60, p. 1906–1917, https://doi.org/10.1080/00206814.2017.1405748.

Lozovskiy, V.R., 1967, New data on the stratigraphy of the Lower Triassic deposits in Moscow syneclise: Digest of Articles on Geology and Hydrogeology (Moscow, Nedra Publishing House), Issue 6, p. 121–128 [in Russian].

Lozovskiy, V.R., and Esaulova, N.K., eds., 1998, Permian-Triassic Boundary in the Continental Series of East Europe: Moscow, GEOS, 246 p.

Lozovskiy, V.R., Balabanov, Y.P., Novikov, I.P., Morkovin, B.I., and Yaroshenko, O.P., 2015, Stratigraphy, palaeomagnetism and petromagnetism of the Lower Triassic in the Moscow syneclise: 2. Vetluga and Unzhi Rivers Basin: Bulletin of the Moscow Society of Naturalists, Geological section, v. 90, no. 2, p. 27–43 [in Russian].

Lucas, S.G., 2017, Permian tetrapod extinction events: Earth-Science Reviews, v. 170, p. 31–60, https://doi.org/10.1016/j.earscirev.2017.04.008.

Metcalfe, I., Crowley, J.L., Nicoll, R.S., and Schmitz, M., 2015, High-precision U-Pb CA-TIMS calibration of Middle Permian to Lower Triassic sequences, mass extinction and extreme climate-change in eastern Australian Gondwana: Gondwana Research, v. 28, p. 61–81, https://doi.org/10.1016/j.gr.2014.09.002.

Molostovskaya, I.I., Naumcheva, M.A., and Golubev, V.K., 2018, Severodvinian and Vyatkian ostracodes from the Suchona River Basin, Vologda region, Russia, *in* Nurgaliev, D.K., ed., Advances in Devonian, Carboniferous and Permian Research: Stratigraphy, Environments, Climate and Resources: Bologna, Italy, Filodiritto Editore, p. 179–187.

Murchison, R.I., de Verneuil, E., and von Keyserling, A., 1845, The Geology of Russia in Europe and the Ural Mountains: London, Murray, https://doi.org/10.5962/bhl.title.121912.

Naumcheva, M.A., and Golubev, V.K., 2020, Nonmarine ostracodes at the Permian-Triassic boundary of the central part of the East European Platform: Palaeoworld, https://doi.org/10.1016/j.palwor.2019.02.001 (in press).

Newell, A.J., Sennikov, A.G., Benton, M.J., Molostovskaya, I.I., Golubev, V.K., Minikh, A.V., and Minikh, M.G., 2010, Disruption of playa-lacustrine depositional systems at the Permo-Triassic boundary: Evidence from Vyazniki and Gorokhovets on the Russian Platform: Journal of the Geological Society [London], v. 167, p. 695–716, https://doi.org/10.1144/0016-76492009-103.

Nielsen, E., 1954, *Tupilakosaurus heilmani* n. g. et n. sp.: Meddelelser om Grønland, v. 72, no. 2, p. 1–33.

Novikov, I.V., 2018, Early Triassic Amphibians of Eastern Europe: Evolution of Dominant Groups and Traits of Changing Communities: Moscow, Russian Academy of Sciences, 358 p. [in Russian].

Ramezani, J., and Bowring, S.A., 2018, Advances in numerical calibration of the Permian timescale based on radioisotopic geochronology, *in* Lucas, S.G., and Shen, S., eds., The Permian Times: Geological Society [London] Special Publication 450, p. 51–60, https://doi.org/10.1144/SP450.17.

Sanson-Barrera, A., Hochuli, P.A., Bucher, H., Schneebeli-Hermann, E., Weissert, H., Adatte, T., and Bernasconi, S.M., 2015, Late Permian–earliest Triassic high-resolution organic carbon isotope and palynofacies records from Kap Stosch (East Greenland): Global and Planetary Change, v. 133, p. 149–166, https://doi.org/10.1016/j.gloplacha.2015.08.006.

Scholze, F., Golubev, V.K., Niedźwiedzki, G., Schneider, J.W., and Sennikov, A.G., 2019, Late Permian conchostracans (Crustacea, Branchiopoda) from continental deposits in the Moscow syneclise, Russia: Journal of Paleontology, v. 93, p. 72–97, https://doi.org/10.1017/jpa.2018.58.

Sennikov, A.G., and Golubev, V.K., 2017, Sequence of Permian tetrapod faunas of Eastern Europe and the Permian-Triassic ecological crisis: Paleontological Journal, v. 51, p. 600–611, https://doi.org/10.1134/S0031030117060077.

Taylor, G.K., Tucker, C., Twitchett, R.J., Kearsey, T., Benton, M.J., Newell, A.J., Surkov, M.V., and Tverdokhlebov, V.P., 2009, Magnetostratigraphy of Permian/Triassic boundary sequences in the Cis-Urals, Russia: No evidence for a major temporal hiatus: Earth and Planetary Science Letters, v. 281, p. 36–47, https://doi.org/10.1016/j.epsl.2009.02.002.

Tohver, E., Lanci, L., Wilson, A., Hansma, J., and Flint, S., 2015, Magnetostratigraphic constraints on the age of the lower Beaufort Group, western Karoo Basin, South Africa, and a critical analysis of existing U-Pb geochronological data: Geochemistry Geophysics Geosystems, v. 16, p. 3649–3665, https://doi.org/10.1002/2015GC005930.

Tverdokhlebov, V.P., Tverdokhlebova, G.I., Minikh, A.V., Surkov, M.V., and Benton, M.J., 2005, Upper Permian vertebrates and their sedimentological context in the South Urals, Russia: Earth-Science Reviews, v. 69, p. 27–77, https://doi.org/10.1016/j.earscirev.2004.07.003.

Wignall, P.B., Sun, Y., Bond, D.P.G., Izon, G., Newton, R.J., Védrine, S., Widdowson, M., Ali, J.R., Lai, X., Jiang, H., Cope, H., and Bottrell, S.H., 2009, Volcanism, mass extinction, and carbon isotope fluctuations in the Middle Permian of China: Science, v. 324, p. 1179–1182, https://doi.org/10.1126/science.1171956.

Yang, J., Cawood, P.A., Du, Y., Condon, D.J., Yan, J., Liu, J., Huang, Y., and Yuan, D., 2018, Early Wuchiapingian cooling linked to Emeishan basaltic weathering?: Earth and Planetary Science Letters, v. 492, p. 102–111, https://doi.org/10.1016/j.epsl.2018.04.004.

Yuan, D.-X., Shen, S.-z., Henderson, C.M., Chen, J., Zhang, H., Zheng, Q.-f., and Wu, H., 2019, Integrative timescale for the Lopingian (Late Permian): A review and update from Shangsi, South China: Earth-Science Reviews, v. 188, p. 190–209, https://doi.org/10.1016/j.earscirev.2018.11.002.

Zakharov, Yu.D., Biakov, A.S., Richoz, S., and Horacek, M., 2015, Importance of carbon isotopic data of the Permian-Triassic boundary layers in the Verkhoyansk region for the global correlation of the basal Triassic layer: Doklady Earth Sciences, v. 460, p. 1–5, https://doi.org/10.1134/S1028334X15010092.

Zhong, Y.-T., He, B., Mundil, R., and Xu, Y.-G., 2014, CA-TIMS zircon U-Pb dating of felsic ignimbrite from the Binchuan section: Implications for the termination age of Emeishan large igneous province: Lithos, v. 204, p. 14–19, https://doi.org/10.1016/j.lithos.2014.03.005.

Printed in USA